ISSN 8755-6839

SCIENCE OF **TSUNAMI HAZARDS**

Journal of Tsunami Society International

Volume 38 Number 1 2019

FAST EVALUATION OF TSUNAMI WAVES HEIGHTS AROUND KAMCHATKA AND KURIL ISLANDS

Mikhail Lavrentiev[1,2], Konstantin Lysakov[1,2], Andrey Marchuk[3], Konstantin Oblaukhov[2,4], and Mikhail Shadrin[1,2]

[1] Institute of Automation and Electrometry SD RAS, 1 Ac. Koptyug pr., Novosibirsk, 630090 Russia
[2] Novosibirsk State University, 1 Pirogov st., Novosibirsk, 630090 Russia
[3] Institute of Computational Mathematics and Mathematical Geophysics SD RAS, 6 Ac. Lavrentiev pr., Novosibirsk, 630090 Russia
[4] "SoftLab-NSK" Ltd, 1 Ac. Koptyug pr., Novosibirsk, 630090 Russia
E-mail addresses: lavrentiev@iae.nsk.su, lysakov@sl.iae.nsk.su, ***mag@omzg.sscc.ru***, *oblaukhov@sl.iae.nsk.su, mikesha@sl.iae.nsk.su*

ABSTRACT

In this paper, we consider the problem of fast wave heights numerical evaluation of hypothetical tsunami along Pacific coast of Kamchatka Peninsula and the Kuril Islands. We focus on PC-based fast numerical calculation of tsunami wave propagation according to the classical shallow water approximation. Valuable performance gain is achieved by using the advantages of the modern computer architectures, namely the Field Programmable Gates Arrays (FPGAs). The Mac-Cormack finite difference scheme of the second order approximation to solve the shallow water system (Titov V. and Gonzalez F. 1997) has been implemented to the FPGA-based Calculator, specially designed by the authors for this task (Lavrentiev et al., 2017; Lysakov et al., 2018). Numerical tests show that it takes only a few seconds to calculate tsunami wave propagation over approximately 2000x2000 km (3120x2400 knots) water area with about 900 m step gridded bathymetry for the given realistic tsunami wave source. The FPGA calculator was also tested on the exact analytical solution obtained by Marchuk (2017) for model bottom topography.

1. INTRODUCTION

Events of a seismic nature following by catastrophic floods caused by a tsunami wave (the instances of which have increased in the last decades) have an important impact on the population of littoral regions. This paper presents the results of numerical simulation to obtain the distribution of tsunami wave heights using the real bathymetry around Kamchatka Peninsula and Kuril Islands. Characteristics of the source, used for numerical experiments, are close to those of disaster event of March 11, 2011 (The Great East Japan Earthquake). Our goal is to reduce the required time for numerical modeling of tsunami wave propagation by using the proposed hardware-software solution, based of the Field Programmable Gates Array (FPGA). The FPGA-based co-processor, in the sequel referred to as Calculator, is installed on a regular PC.

As is well known, DART (Deep-ocean Assessment and Reporting of Tsunami) buoys, (see https://nctr.pmel.noaa.gov/Dart/) or any other pressure sensor system, like the DONET (Dense Oceanfloor Network system for Earthquakes and Tsunamis) (https://www.jamstec.go.jp/donet/e/), provide measurements of the passing tsunami wave in the real-time mode. So, the measured wave profile is available in real time (even just as the wave is passing over the sensor) through the satellite network channels. Having these measured data, first, it is necessary to recalculate the detected wave profile in terms of the initial sea surface displacement at tsunami source. There are different approaches to do this, see (Hiroaki T. and Yusaku O., 2014; Voronina T., 2016), e.g. We would like to refer also to the “orthogonal decomposition” approach, see (Lavrentiev M., Kuzakov D. et al., 2017; 2018). The corresponding algorithm works very fast estimating the initial water surface displacement at a source in a few seconds with just a regular PC.

Fast calculation of tsunami wave heights distribution along the entire coastal line under study would be really helpful for the local authorities to make a decision about the necessary safety measures to avoid casualties and to reduce economy loss. Calculation of the wave propagation over the given water area is now a rather standard process, based on numerical solution to linear or nonlinear shallow water differential equations. The USA NOAA tsunami warning centers use the so-called MOST (Method Of Splitting Tsunamis) software package, which simulates all tsunami phases – generation, propagation, and inundation of the dry land, see (Titov V. and Gonzalez F. 1997). Here we address the module of MOST software, responsible for calculation of the wave propagation only. As was proved in numerical mathematics, one can trust numerical solution to evolution type system of partial differential equations only if the time step is in a certain relation with the space grid step length. Therefore, calculation with the fine enough computational grid, may require too much time even with an advanced computer. So, one of the possible ways to carry out in time the wave propagation computation from a source up to a shoreline, is nested grids algorithms (Hayashi K. et al., 2015). The second way is using the modern computer architectures like Graphic Processing Unit (GPU) or FPGA microchip.

Presently, most of performance gain is due to the parallel implementation of a given data processing algorithms. Such parallel calculations require the corresponding hardware, namely multi-core CPU clusters (rather expensive within supercomputing units), GPU based hybrid systems, or FPGA microchip based special processors. Using FPGA microchip advantages, we accelerate solution to system of shallow water equations. The achieved performance at regular PC with the proposed Calculator is nearly 250 times faster compared to propagation of the real wave (6 sec against 1600 sec).

The rest of the paper is as follows. We first present a version of shallow water system, used for numerical computations and the description of the Mac-Cormac numerical scheme. Comparison of numerical solution with the analytic one for model bathymetry is also given. In the next section the proposed Calculator – hardware device for code execution acceleration, is briefly described. Then the results of a number of numerical tests, arranged at the real digital bathymetry with 30 arc sec (nearly 900 m) mesh step are presented. We use the initial seabed displacement at tsunami source similar to those of the Great Tohoku Earthquake of 2011. Obtained numerical results are then discussed.

2. MATHEMATICAL STATEMENT OF THE PROBLEM

The referred software package MOST (like many other tools) uses the following equivalent form of a shallow water system (which does not take into account such external forces as sea bed friction, Coriolis force and others), which could be found in (Titov V. and Gonzalez F. 1997):

$$H_t + (uH)_x + (vH)_y = 0,$$

$$u_t + uu_x + vu_y + gH_x = gD_x, \qquad (1)$$

$$v_t + uv_x + vv_y + gH_y = gD_y,$$

where $H(x, y, t)=\eta(x, y, t)+D(x, y, t)$ is the entire height of water column, $\eta(x,y,t)$ being the sea surface disturbance (wave height), $D(x,y)$ – depth (which is supposed to be known at all grid points), u and v components of water flow velocity vector, g – acceleration of gravity.

The so-called Mac-Cormack scheme (MacCormack R. and Paullay A., 1972) was used for numerical treatment of the shallow water system (1). The Mac-Cormack algorithm is a direct difference scheme at three-point stencil of a "cross" type. Simulation domain is assumed to be a fixed rectangle (respectively to geographic coordinates), time independent:

$$\Omega((x,y) = \{(x,y): X_1 \le x \le X_2,\ Y_1 \le y \le Y_2,\ X_i,\ Y_j \text{ - } const\}.$$

The uniform rectangle grid is considered in Ω:

$$\overline{\Omega}(x,y) = \{((x_i,y_j): X_1 \le x_i \le X_2,\ Y_1 \le y_j \le Y_2, 0 \le i \le N_x,\ 0 \le j \le N_y\},$$

where $\Delta x = x_{i+1} - x_i$, $\Delta y = y_{i+1} - y_i$ – grid steps with respect to variables x and y, respectively. Consider the partition of the time period for wave propagation:

$$\bar{\gamma} = \{(t^n): 0 \le n \le N_t\}$$

$\tau^n = t^{n+1} - t^n$ – time steps. For simplicity, in the sequel we use a uniform step $\tau^n = \tau$, while, in case of necessity, it is not a problem to use the variable time steps. We will use standard notation for the mesh variables Φ at node *(i,j)*, as $\Phi_{ij}^n = \Phi(x_i, y_j, t^n)$.

The shallow water equations (1) at the mesh nodes $\overline{\Omega}$ on the *n*-th time step will be approximated with the help of explicit two-steps Mac-Cormack finite difference scheme of the second order approximation:

1st step:

$$\frac{\widehat{H}_{ij}^{n+1} - H_{ij}^n}{\tau} + \frac{H_{ij}^n u_{ij}^n - H_{i-1j}^n u_{i-1j}^n}{\Delta x} + \frac{H_{ij}^n v_{ij}^n - H_{ij-1}^n v_{ij-1}^n}{\Delta y} = 0,$$

$$\frac{\widehat{u}_{ij}^{n+1} - u_{ij}^n}{\tau} + u_{ij}^n \frac{u_{ij}^n - u_{i-1j}^n}{\Delta x} + v_{ij}^n \frac{u_{ij}^n - u_{ij-1}^n}{\Delta y} + g \frac{\eta_{ij}^n - \eta_{i-1j}^n}{\Delta x} = 0, \quad (2)$$

$$\frac{\widehat{v}_{ij}^{n+1} - v_{ij}^n}{\tau} + u_{ij}^n \frac{v_{ij}^n - v_{i-1j}^n}{\Delta x} + v_{ij}^n \frac{v_{ij}^n - v_{ij-1}^n}{\Delta y} + g \frac{\eta_{ij}^n - \eta_{ij-1}^n}{\Delta y} = 0.$$

2nd step:

$$\frac{H_{ij}^{n+1} - \left(\widehat{H}_{ij}^{n+1} + H_{ij}^n\right)/2}{\tau/2} + \frac{\widehat{H}_{i+1j}^{n+1}\widehat{u}_{i+1j}^{n+1} - \widehat{H}_{ij}^{n+1}\widehat{u}_{ij}^{n+1}}{\Delta x} + \frac{\widehat{H}_{ij+1}^{n+1}\widehat{v}_{ij+1}^{n+1} - \widehat{H}_{ij}^{n+1}\widehat{v}_{ij}^{n+1}}{\Delta y} = 0,$$

$$\frac{u_{ij}^{n+1} - \left(\widehat{u}_{ij}^{n+1} + u_{ij}^n\right)/2}{\tau/2} + u_{ij}^n \frac{\widehat{u}_{i+1j}^{n+1} - \widehat{u}_{ij}^{n+1}}{\Delta x} + v_{ij}^n \frac{\widehat{u}_{ij+1}^{n+1} - \widehat{u}_{ij}^{n+1}}{\Delta y} + g \frac{\widehat{\eta}_{i+1j}^{n+1} - \widehat{\eta}_{ij}^{n+1}}{\Delta x} = 0, \quad (3)$$

$$\frac{v_{ij}^{n+1} - \left(\widehat{v}_{ij}^{n+1} + v_{ij}^n\right)/2}{\tau/2} + u_{ij}^n \frac{\widehat{v}_{i+1j}^{n+1} - \widehat{v}_{ij}^{n+1}}{\Delta x} + v_{ij}^n \frac{\widehat{v}_{ij+1}^{n+1} - \widehat{v}_{ij}^{n+1}}{\Delta y} + g \frac{\widehat{\eta}_{ij+1}^{n+1} - \widehat{\eta}_{ij}^{n+1}}{\Delta y} = 0.$$

Usually, the real tsunami wave simulation is performed in a spherical or geodetic coordinate system (λ,φ), where λ is the longitude and φ is the latitude in arc degrees. Accordingly, the following relations are used to calculate the differences Δx and Δy:

$$\Delta x_{ij} = \frac{\pi(\lambda_{i+1} - \lambda_i)}{180°} R_E \cos(\varphi_j),$$

$$\Delta y_{ij} = \frac{\pi(\varphi_{i+1} - \varphi_i)}{180°} R_E,$$

where R_E stands for the Earth radius. This scheme looks similar to the splitting method (with respect to space variables), which is used in the MOST software package. Indeed, in order to calculate the values of the sought functions at grid-point *(i,j,n+1)* the values at 3 points of the previous time step *(i,j,n) (i-1,j,n) (i,j-1,n)* are used during the first half-step in (2), and the values at the points *(i,j,n) (i+1,j,n) (i,j+1,n)* during the second half-step in (3). However, comparison of the known analytic solutions with the numerically obtained ones show that the proposed attempt to realize the three-points calculation stencil (Mac-Cormack scheme) seems to be preferable compared to the one from the MOST software package (Lavrentiev et al., 2017; Lysakov et al., 2018).

Indeed, precision of the proposed implementation of the Mac-Cormack scheme has been tested by a comparison of the computed solution with the known analytic solutions for the model case of the parabolic bottom topography, see (Marchuk An., 2017). The 1000 * 1000 km littoral area was considered, where the depth increases according to the formula:

$$D(x,y)=10^{-8}\cdot y^{2},$$

where the ordinate *y* means the distance to the coastline. As is observed in Fig. 1, the achieved precision is the same or better, as compared to the MOST software package.

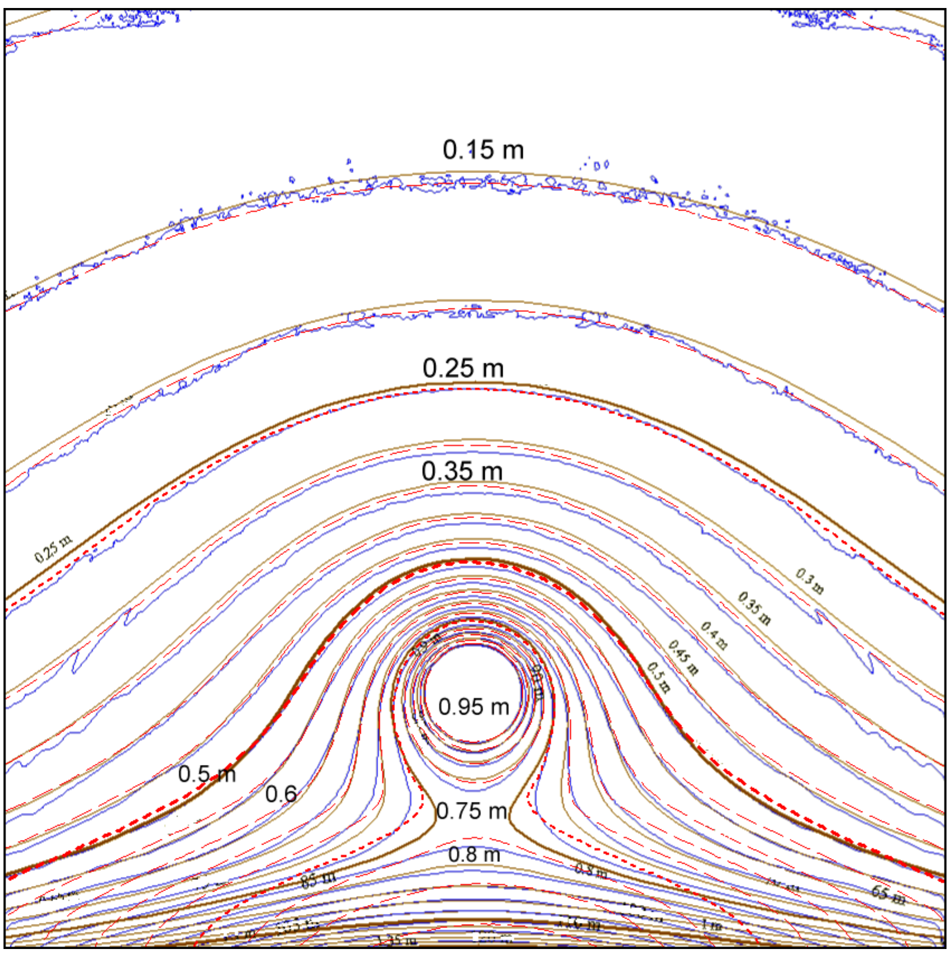

Figure 1. Comparison of the wave height maxima distribution obtained within ray approximation (brown isolines) with results of numerical modelling using FPGA calculator (red isolines) and by the MOST software (blue isolines).

3. FPGA BASED CALCULATOR

Modern Field Programmable Gate Array (FPGA) microchips provide the possibility of parallel implementation of hundreds of thousands of simultaneous computation flows; their internal memory attains tens of megabits. FPGAs are configurable processors, i.e., the same hardware device may serve as a special processor for different tasks, depending on a particular loaded algorithm. This platform makes it possible to construct the computational architecture the most suitable for the implemented algorithms. Moreover, FPGA microchips can be reconfigured an unlimited number of times to solve different problems or change processing algorithm.

According to difference scheme (2)-(3), at each grid-point it is necessary to calculate the values of three grid-functions: H_{ij}^{n+1}, u_{ij}^{n+1}, and v_{ij}^{n+1}. For the FPGA algorithm implementation, the stream processor architecture was proposed. It consists of a certain processor elements (PEs). Such PEs executes a version of a 2-dimension run, a pipeline with a sequential data stream. The auxiliary data for each node required to be stored in memory, are the values of all functions in use at 4 neighbor nodes forming computation stencil. The FPGA architecture makes it possible to use the fast inner memory (BRAM) for implementing such stencil buffer.

The input data flow is a sequential line-by-line inspection of all the grid points. The suggested PE architecture allows either processing several points simultaneously, or connecting in series several PEs to implement several iterations as a single pipeline. This makes it possible to optimize the PE set according to the peculiarities of a given hardware platform. The mathematical operations in (2), (3) of Mac-Cormack difference scheme are implemented as a calculation pipeline, with performance of 1 node treatment at one computer clock cycle.

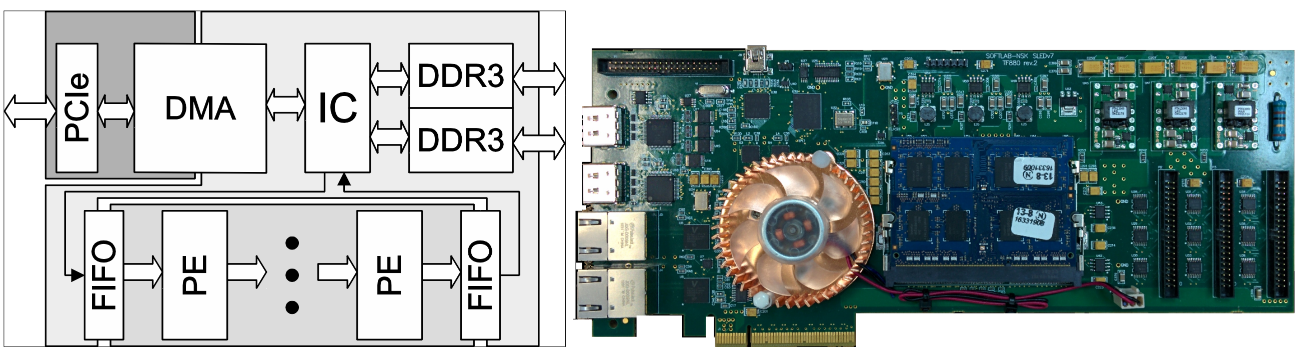

Figure 2. Operation scheme and appearance of the FPGA based Calculator.

Block-scheme of the Calculator and its appearance are given in Fig. 2. In addition to Processing Elements (PE's), which perform calculation in parallel mode, the Calculator has memory controllers DDR3, PCIe controller, and DMA modulus responsible for the direct access to the host computer memory. The Calculator receives the input data from the memory through FIFO (First In, First Out) memory, which makes it possible to adopt the frequency of separate calculation modules tuning it to the particular FPGA microchip as well as the outer memory and interface characteristics. Calculator may contain several PEs, depending on the characteristics of a particular FPGA in use. Block-scheme of the Calculator, based of FPGA microchip Xilinx Virtex-7 VC709, is available in (Lavrentiev et al., 2017; Lysakov et al., 2018).

Let us give some explanations about calculation pipeline realized in this FPGA based Calculator. Recent version contains 16 Processing Elements (PEs). The sequence of tasks is arranged as follows. The first couple of PEs works on calculation of the tsunami flow parameters corresponding to the time layer *n+1*. Both PEs use the digital bathymetry array depth values and wave parameters on the previous time layer only along 3 lines of computational domain which are enough for obtaining values of H_{ij}^{n+1}, u_{ij}^{n+1}, v_{ij}^{n+1} ($i=1,..,N_x$) along the certain line *j* of rectangle grid $\overline{\Omega}$. First PE obtains values on the intermediate time layer *n+1/2*, which are used by the second PE for the almost simultaneous calculating of wave parameters for time layer *n+1*. Then this couple of PEs takes into account wave parameters H_{ij}^{n}, u_{ij}^{n}, v_{ij}^{n} ($i=1,..,N_x$) and the depth along the next line *j+2* of computational domain, where the values for time layer *n+1* along the grid line *j+1* must be calculated. So, line-by-line the first couple of PEs calculates and sends to DMA the wave parameters for time layer *n+1*. When these tsunami parameters have been obtained (with the help of first couple of PEs) for first 3 grid lines of domain, then the second couple of PEs starts calculating wave parameters for time layer *n+2*. After the first 3 lines have been completed by the second couple of PEs the third couple starts to work on the time layer *n+3*, and so on. After completing the time layer *n+1* by the first couple of PEs, it starts processing grid variables for time layer *n+9*. This pipeline cycle continues up to the numerical experiment number of time steps limit. The FPGA calculator simultaneously works on wave parameters at 8 time layers with 3 grid lines delay each.

4. NUMERICAL EXPERIMENTS

Numerical experiments were arranged at the gridded bathymetry around Kamchatka Peninsula and Kuril Islands, visualization of which is presented in Fig.3. This 30 arc sec resolution gridded bathymetry was developed in Bezhaev, Marchuk and Seliverstov (2002) based on the large number of depth soundings provided by “Vulkanolog” vessel. For ocean depth description in far-field areas the segments of global digital bathymetry database developed in (Smith and Sandwell, 1997) have been added. This digital bathymetry and computational grid have the following characteristics:

- Grid size is 3120x2400 points
- Grid steps are 30 arc seconds in both directions (which means approximately 584 and 928 meters, respectively);
- Array covers the area between 144° and 170° E, 41° and 61° N;
- Time step used in computations is equal to 1.0 sec.

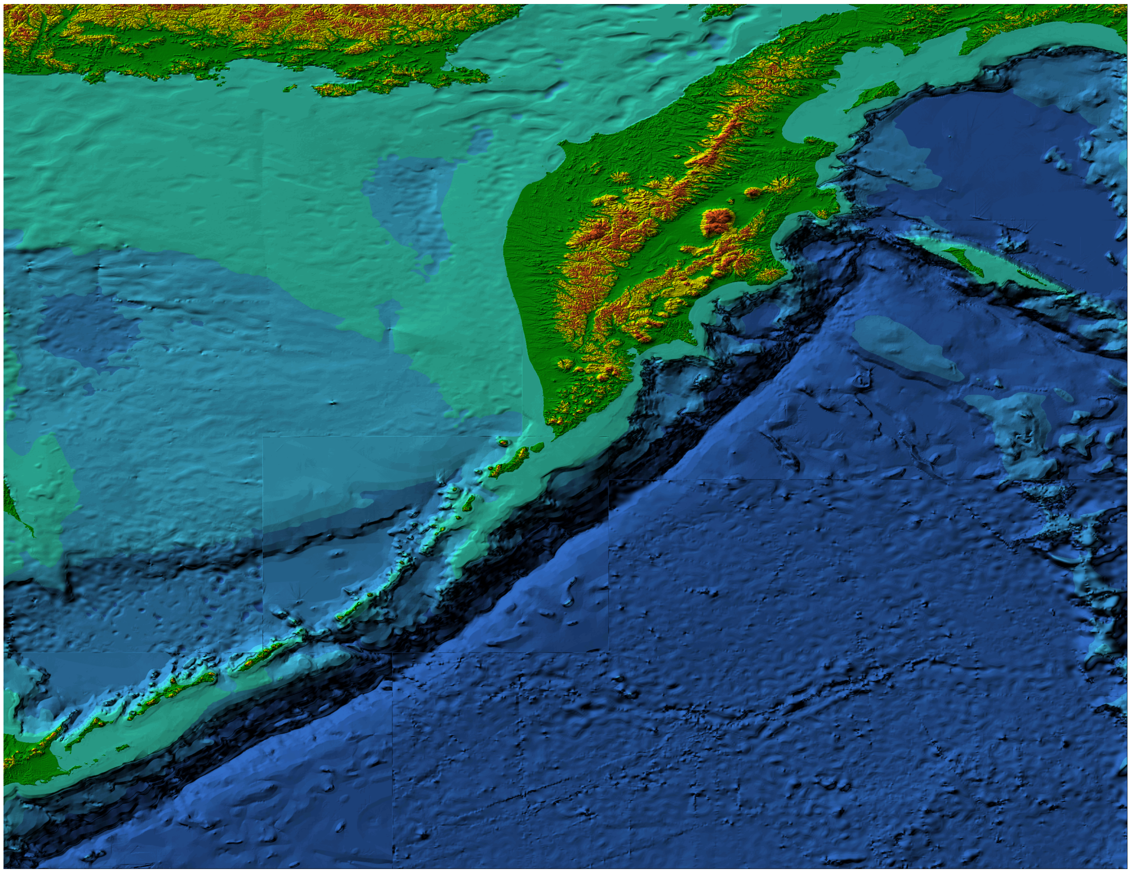

Figure 3. Digital bathymetry of the Russian Far-East Kuril-Kamchatka region.

The FPGA based Calculator with a regular modern PC needs 24 sec to simulate the first 90 minutes of the wave propagation from the dipole-type source. This source looks similar to the unit source used for tsunami forecast by NOAA (Gica E. et al., 2008) but significantly stretched in one direction. The shape and profile of the typical unit source is based on the available geological and geophysical information. Due to this, the typical for subduction zone seabed displacement area for 7.5 M earthquake was approximated by 50x100 km rectangle having maximum water surface elevation as 57 cm. The initial seabed displacement at such a unit source is shown in Fig. 4.

Figure 4. 2D shaded and 3D views of the source used for numerical modeling.

The extended 500 km long model tsunami source was used in numerical experiment. The source size has the same order as 1952 Kamchatka and 2011 Great Tohoku tsunami sources but the maximum initial water surface elevation at source is taken equal to +200 cm. Geographic location of this source is shown in Fig. 5 as two ellipses. The part of source with the initial surface depression is located closer to the coast than the uplift wing. The "real" propagation time for the wave in this case is evaluated as 6000 sec. This includes wave approaching and reflecting off the shore processes.

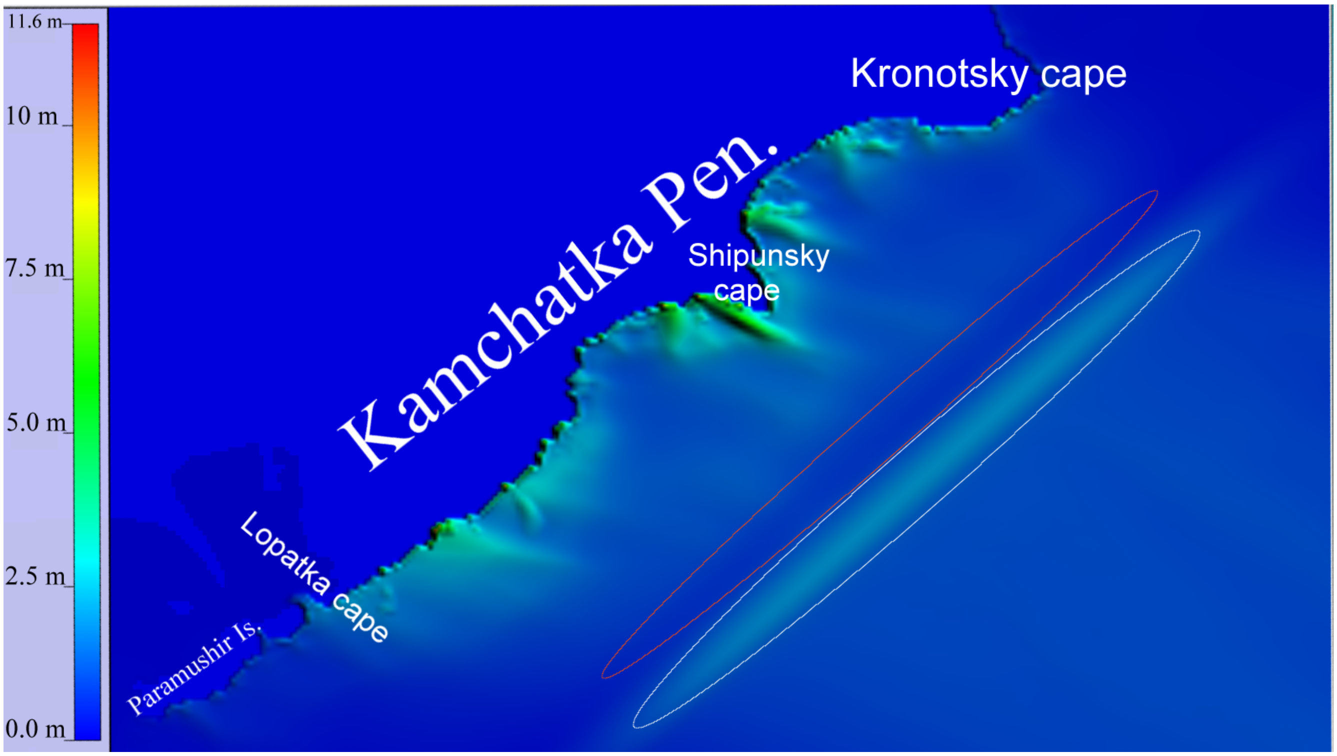

Figure 5. Position of model tsunami source eastward of Kamchatka peninsular and distribution of the wave maxima near the Northern Kuril and Kamchatka coast.

Numerical simulation with the 3120x2400 nodes computational grid shows that the main wave approaches the nearest shore in approximately 1600 sec after the shock. With the proposed FPGA based Calculator, it takes only a few seconds to calculate the maximal height distribution along the entire coastline considered. Namely, it takes 29.95 sec for the Calculator based on Virtex-6 microchip (SLEDv7 printed board), while just 5.98 sec with VC709 microchip. The similar computational experiment was carried out using MOST software. It takes not less than 1.0 sec for calculating each time step on the medium class PC (2.5-3.0 GHz). In the other words, it takes approximately 1800 sec for calculation with the MOST software tsunami propagation up to the nearest coast. So, the performance gain, achieved by the proposed Calculator, is nearly 250 times compared to the MOST software. It means that calculation is executed at least 250 times faster compared to propagation of the real wave (6 sec against 1600 sec).

Figure 6 shows the more detailed FPGA computed distribution of tsunami wave maxima along the North Kurils and Kamchatka shore for the tsunami source under study.

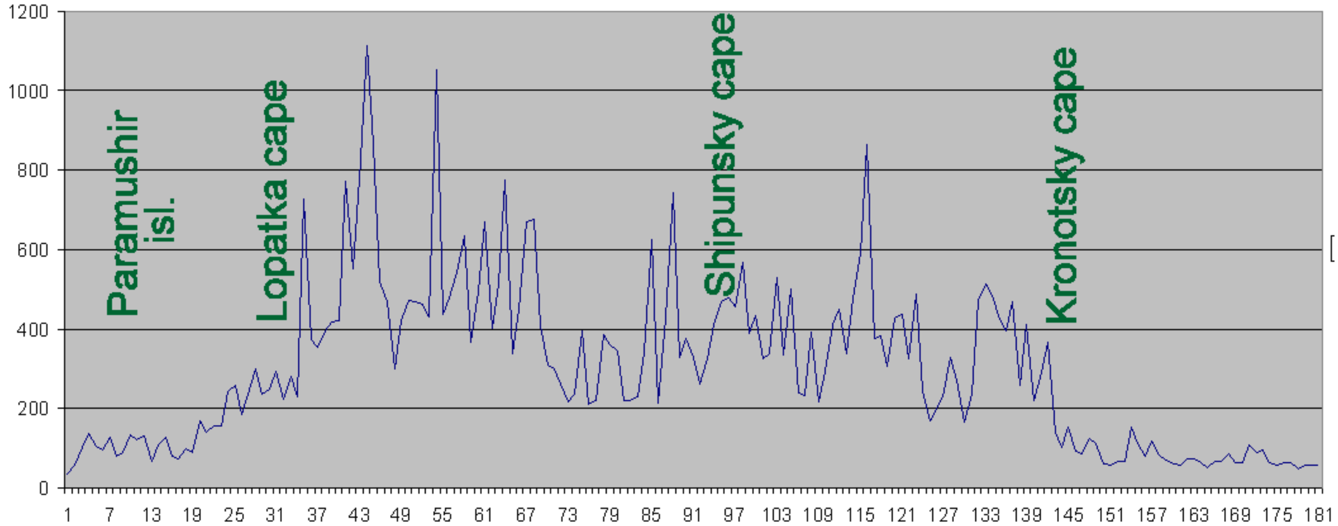

Figure 6. Distribution of tsunami wave maxima (in centimeters) along North Kurils and Kamchatka shore obtained with FPGA based Calculator.

This wave-height distribution shows that for such location of the initial sea surface displacement (Fig. 5) the highest tsunami waves (up to 12 m) are expected at some harbors in the southern part of Kamchatka Peninsula. At the coastline areas, which are not just opposite to the described source, the height of tsunami is significantly lower (100-200 cm only). It is comparable to the maximal vertical displacement at tsunami source. In order to verify numerical results, obtained with the described FPGA based Calculator, the same numerical experiment was carried out using MOST software. Fig. 7 below presents the computed maximal heights of tsunami wave generated by the same extended source, which is shown in Fig. 4.

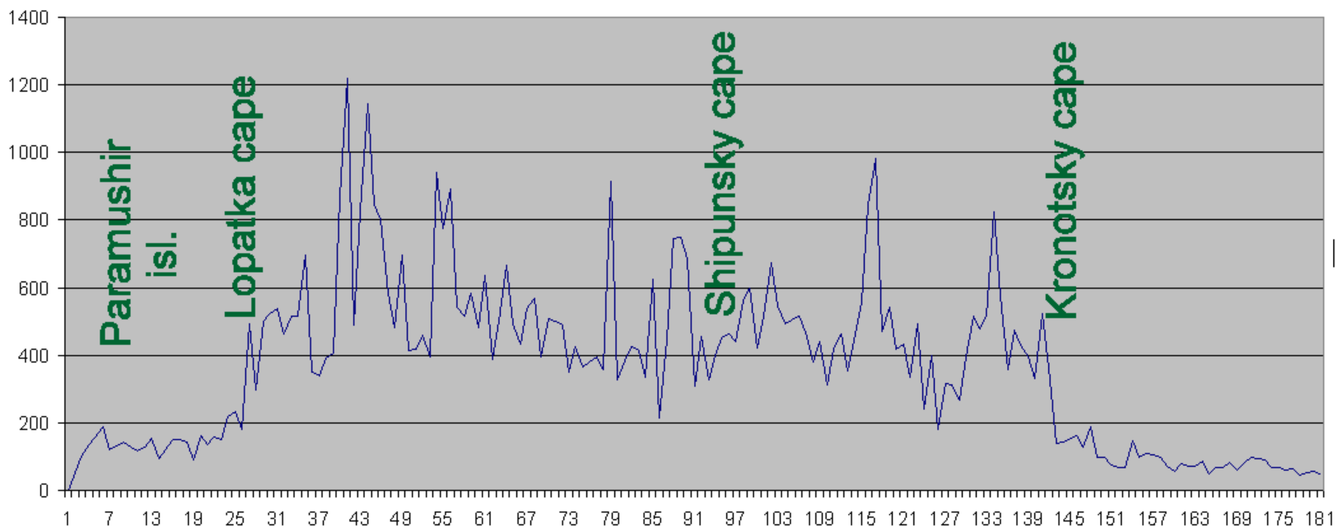

Figure 7. Distribution of tsunami wave maxima along the shore calculated by MOST software.

As is observed from the Fig. 7, the maximum tsunami heights distribution along the North Kurils and Kamchatka coast is similar to the one obtained using FPGA based Calculator. This comparison proves reliability of numerical results obtained with FPGA based Calculator, which can be obtained within few seconds after start of calculation. Let compare this processing time to hours required for computation using MOST software.

Now, let us say few words about the digital bathymetry, used for numerical tests. Usually, the grid step is determined by the available bathymetry databases, accounting for the goals of numerical modeling. These days such grid step, typically about 900 m, is considered too large. However, it depends on the modeling goals. When one needs a detailed evaluation of the expected wave heights along the entire shoreline, it is necessary to carry out numerical modeling with the corresponding fine mesh size in the near-coast regions. It could be done by choosing the properly small grid step in the entire water area. However, the number of computational nodes will increase by 2-3 orders, which results in the necessity of extended computational facilities or, alternatively, in a dramatic increase of the CPU time required for simulation. As for the proposed FPGA-based Tsunami Wave Calculator, the available memory resources dictate the limit of approximately 50 millions for a number of computational nodes.

There is even a more important challenge. Refining a computational grid using interpolation of depth values to 10-20 m resolution will miss the fine details of real bathymetry, which are not reflected in the original 900 m resolution database. Therefore, results of numerical modeling will be rather far from reality in the near shore areas. Natural solution to this problem could be obtained by the nested grids approach, where the resolution depends, roughly speaking, on the distance to the shore. Of course, the fine digital bathymetry in the coastal area is required for obtaining the detailed wave height distribution along the shoreline. A combination of the nested grids approach with the hardware code acceleration (by the use of Graphic Processing Units – GPU) has been tested by the authors simulating tsunami wave propagation at Sanriku coast, see (Hayashi K. et al., 2015).

When the fine digital bathymetry in the coastal area is available, it is not a problem to pass the obtained numerically wave parameters from the original «rough gridded» area to the one with a fine grid. The algorithm in use admits simultaneous computations in several near-coast areas. So, by using just a few of the proposed FPGA based Calculator, PCs gives ability for Tsunami Warning Centers (services) to obtain the robust evaluation of maximal tsunami wave heights along the entire coastal region by the reasonably short time, certainly much less compared to the wave travel time from the source to the coast.

5. DISCUSSION

Having such tool as the designed “Tsunami Wave” Calculator, operating with the regular PC as a co-processor, it is possible to move toward the real-time instrument for the local authorities to evaluate tsunami danger in any particular part of the coast. Indeed, shortly after strong near shore underwater seismic event the magnitude and epicenter location is known. In case the event could be dangerous, special service (municipal, e.g.) can order (and certainly pick up) the time series – tsunami wave profile, measured by available sensor system (DONET, S-NET, DART buoy, or any other). Rather simple algorithm, see (Lavrentiev M., Kuzakov D. et al., 2017; 2018) will recalculate these data in terms of the initial seabed (sea surface) displacement at tsunami source just in a few seconds. Then, using the Calculator, any expert is able to calculate an approximation of the expected wave height distribution along the valuably long part of the coast. As the computation takes less then a minute, several scenarios (differ from each other by small shifts of the initial displacement area) could be processed. Short calculation time gives possibility to use longer wave time series for reconstruction tsunami source which must improve the final height prediction. This would provide a solid ground for decision makers for evacuation measures.

After development and testing of a number of the real time algorithms, covering the entire process, namely: automated order of tsunami wave profile from the sensor network, automated accounting of the tidal component, wave profile recalculation in terms of the initial sea bed displacement at tsunami source, generation of adaptive digital bathymetry, calculation of tsunami wave propagation, inundation mapping, it will be possible to create the real time decision support software for tsunami warning services.

6. CONCLUSION

As a step toward the real-time tsunami danger evaluation, the FPGA-based specialized Calculator has been designed and tested. It uses FPGA microchip, which dramatically accelerates numerical modeling of tsunami wave propagation. Calculation of the tsunami wave propagation from the hypothetic source up to the Kuril-Kamchatka shoreline in the 3120x2400 knots computational domain takes only a few seconds. So, the wave height distribution along the coast can be determined almost immediately after restoration of the initial water surface displacement at the tsunami source area. As was shown earlier, the precision of numerical results is the same then using the MOST software, the official tool of NOAA (USA) tsunami warning centers. These results show the possibility of tsunami danger forecast in the real-time mode. The authors will propose soon a version of software which uses nested grids approach to obtain characteristics of a tsunami wave along the detailed shoreline.

7. ACKNOWLEDGEMENTS

This study was supported, in part, by the project 0319-2018-0010 IV.36.1.4. Investigation and development of methods and technologies for construction of integrated software-hardware systems to modeling and control of dynamical systems for data processing and presenting, registration number AAAA-A17-117062110016-4, Institute of Automation and Electrometry SB RAS.

REFERENCES

DART® (Deep-ocean Assessment and Reporting of Tsunamis) [Electronic resource]: https://nctr.pmel.noaa.gov/Dart/

DONET (Dense Oceanfloor Network System for Earthquakes and Tsunamis) [Electronic resource]: https://www.jamstec.go.jp/donet/e/

Gica E., Spillane M.C., Titov V.V., Chamberlin C.D., Newman J.C. Development of the Forecast Propagation Database for NOAA's Short-Term Inundation Forecast for Tsunamis (SIFT), *NOAA Technical Memorandum OAR PMEL-139, Pacific Marine Environmental Laboratory*, Seattle, WA, March 2008.

Hayashi K., Vazhenin A.P., Marchuk An.G. Trans-Boundary Realization of the Nested-Grid Method for Tsunami Propagation Modeling. *Proceedings of the Twenty-fifth (2015) International Ocean and Polar Engineering Conference.* Kona, Big Island, Hawaii, USA, June 21-26, V. 3, International Society of Offshore and Polar Engineers (ISOPE), pp. 741-747. 2015.

Hiroaki T., Yusaku O. Review on Near-Field Tsunami Forecasting from Offshore Tsunami Data and Onshore GNSS Data for Tsunami Early Warning. *Journal of Disaster Research* V. 9 No. 3, pp. 339-357. 2014.

Lavrentiev M.M., Kuzakov D., Romanenko A.A., Vazhenin A.P. Determination of Initial Tsunami Wave Shape at Sea Surface. *Oceans'17 MTS/IEEE, Aberdeen, June 19-22*, 2017

Lavrentiev M.M., Kuzakov D., Marchuk An.G. Determination of Initial Sea Surface Displacement at Tsunami Source by a Part of Wave Profile. *Oceans'18 MTS/IEEE, Kobe, Japan, May 28-31*, 2018.

Lavrentiev M.M., Romanenko A.A., Oblaukhov K.K., Marchuk An.G., Lysakov K.F., Shadrin M.Yu. FPGA Based Solution for Fast Tsunami Wave Propagation Modeling. *The 27th International Ocean and Polar Engineering Conference, 2017, 25-30 June, San Francisco, California, USA* pp 924-929. 2017.

Lysakov K.F., Lavrentiev M.M., Oblaukhov K.K., Marchuk An.G., Shadrin M.Yu. FPGA-based Modelling of the Tsunami Wave Propagation at South Japan Water Area. *Oceans'18 MTS/IEEE, Kobe, Japan, May 28-31*, 2018.

MacCormack R.W., Paullay A.J. Computational Efficiency Achieved by Time Splitting of Finite-Difference Operators. *AIAA paper*. – 1972. – No. 72-154.

Marchuk An.G. Benchmark solutions for tsunami wave fronts and rays. Part 2: Parabolic bottom topography. *SCIENCE OF TSUNAMI HAZARDS*, Vol. 36, No 2, 2017, pp. 70-85.

Marchuk An.G., Bezhaev A.Yu. and Seliverstov N.I. New gridded digital bathymetry for the Kuril-Kamchatka region. *Recent Advances in Marine Science and Technology' 2002, USA, Honolulu, Narendra K. Saxena Editor, PACON International, P.O/ Box 11568, Honolulu, Hawaii 96828 USA*, 2002. (http://nippon.zaidan.info/seikabutsu/2002/00223/contents/044.htm)

Smith W.H.F. and Sandwell D. Global seafloor topography from satellite altimetry and ship depth soundings. *Science* 1997, 277: pp. 1956-1962.

Titov V.V., Gonzalez F.I. Implementation and testing of the method of splitting tsunami (MOST) model. *NOAA Technical Memorandum ERL PMEL-112*, 1997

Voronina T.A. Recovering a tsunami source and designing an observational system based on an *r*-solution method. *Numerical Analysis and Applications* V. 9, No. 4. pp. 267–276. 2016.